Spatiotemporally Controlled Ablation of *Klf5* Results in Dysregulated Epithelial Homeostasis in Adult Mouse Corneas

Chelsea L. Loughner,[*,1] Anil Tiwari,[1] Doreswamy Kenchegowda,[†,1] Sudha Swamynathan,[1] and Shivalingappa K. Swamynathan[1–4]

[1]Department of Ophthalmology, University of Pittsburgh School of Medicine, Pittsburgh, United States
[2]McGowan Institute of Regenerative Medicine, University of Pittsburgh, United States
[3]Department of Cell Biology, University of Pittsburgh School of Medicine, Pittsburgh, United States
[4]Fox Center for Vision Restoration, University of Pittsburgh School of Medicine, Pittsburgh, United States

Correspondence: Shivalingappa K. Swamynathan, University of Pittsburgh School of Medicine, Eye and Ear Institute, 203 Lothrop Street, Room 1025, Pittsburgh PA 15213, USA;
swamynathansk@upmc.edu.

Current affiliation: *Lake Erie College of Osteopathic Medicine, Greensburg, Pennsylvania, United States. †Armed Forces Radiobiology Research Institute, Bethesda, Maryland, United States.

Submitted: June 27, 2017
Accepted: August 14, 2017

Citation: Loughner CL, Tiwari A, Kenchegowda D, Swamynathan S, Swamynathan SK. Spatiotemporally controlled ablation of *Klf5* results in dysregulated epithelial homeostasis in adult mouse corneas. *Invest Ophthalmol Vis Sci*. 2017;58:4683–4693. DOI: 10.1167/iovs.17-22498

Purpose. Corneal epithelial (CE) homeostasis requires coordination between proliferation and differentiation. Here we examine the role of cell proliferation regulator Krüppel-like factor 5 (Klf5) in adult mouse CE homeostasis.

Methods. *Klf5* was ablated in a spatiotemporally restricted manner by inducing Cre expression in 8-week-old ternary transgenic *Klf5*$^{LoxP/LoxP}$/*Krt12*$^{rtTA/rtTA}$/*Tet-O-Cre* (*Klf5*$^{\Delta/\Delta CE}$) mouse CE by administering doxycycline via chow. Normal chow-fed ternary transgenic siblings served as controls. The control and *Klf5*$^{\Delta/\Delta CE}$ corneal (1) histology, (2) cell proliferation, and (3) Klf5-target gene expression were examined using (1) periodic acid Schiff reagent-stained sections, (2) Ki67 expression, and (3) quantitative PCR and immunostaining, respectively. The effect of KLF4, KLF5, and OCT1 on gastrokine-1 (*GKN1*) promoter activity was determined by transient transfection in human skin keratinocyte NCTC-2544 cells.

Results. *Klf5* expression was decreased to 23% of the controls in *Klf5*$^{\Delta/\Delta CE}$ corneas, which displayed increased fluorescein uptake, downregulation of tight junction proteins Tjp1 and Gkn1, desmosomal Dsg1a, and basement membrane Lama3 and Lamb1, suggesting defective permeability barrier. In transient transfection assays, KLF5 and OCT1 synergistically stimulated *GKN1* promoter activity. *Klf5*$^{\Delta/\Delta CE}$ CE displayed significantly fewer cell layers and Ki67^{+} proliferative cells coupled with significantly decreased cyclin-D1, and elevated phospho(Ser-10) p27/Kip1 expression. Expression of Krt12, E-cadherin, and β-catenin remained unaltered in *Klf5*$^{\Delta/\Delta CE}$ corneas.

Conclusions. Klf5 contributes to adult mouse CE homeostasis by promoting (1) permeability barrier function through upregulation of Tjp1, Gkn1, Dsg1a, Lama3, and Lamb1, and (2) basal cell proliferation through upregulation of cyclin-D1 and suppression of phospho(Ser-10) p27/Kip1, without significantly affecting the expression of epithelial markers Krt12, E-cadherin, and β-catenin.

Keywords: Klf5, Klf4, corneal epithelium, proliferation, differentiation, tight junction, desmosome

The cornea is the outermost transparent tissue layer of the eye. It provides a bulk of the refractive power of the eye while protecting the rest of the eye from external insults. Structurally, the mouse cornea consists of an anterior stratified corneal epithelium (CE) that is continuously renewed throughout life, central collagenous stroma populated by keratocytes, and a posterior endothelial monolayer. Diverse factors including abundantly expressed corneal crystallins,[1,2] uniformly ordered stromal collagen fibrils,[3] and active mechanisms that ensure corneal angiogenic and immune privilege[4–7] contribute toward corneal transparent and refractive properties. The mature mouse CE consists of six to eight cell layers composed of the innermost columnar basal cells, suprabasal and medial wing cells, and outermost superficial cells, each with distinct properties.[8] The structural integrity of the CE depends on a diverse range of cell junction complexes. While the most superficial cells display tight junctions that provide a barrier against foreign substances, wing cells are connected by adherens junctions and desmosomes, and the basal cells are anchored on a basement membrane consisting of randomly arranged collagen fibrils and laminins through hemidesmosomes.[8]

During development, CE cell proliferation, migration, and differentiation are tightly regulated by a network of transcription factors.[9] Once formed, the CE is continuously renewed as the most superficial cells are lost by sloughing. Mature CE homeostasis depends on diverse proteins, such as neurokinin-1 receptor, Aldh3a1, clusterin, Shp2, Tsp-1, and Wnt7a, and is regulated by transcription factors, such as Lhx2, Pax6, AP2, EHF, Klf4, and Klf5.[9–19] Disruptions in CE homeostasis are associated with ocular surface disorders, such as dry eye disease, Meesmann's dystrophy, and ocular cicatricial pemphi-

goid.[20–22] Despite its central role in ensuring corneal transparence and refractive properties, molecular mechanisms that coordinate the mature CE homeostasis are not completely understood.

Previously, we demonstrated that the Krüppel-like factors Klf4 and Klf5, abundantly expressed in the mouse cornea,[23] play critical nonredundant roles in the ocular surface and are important nodes in the network of transcription factors that regulate ocular surface maturation.[24,25] Klf4 and Klf5 possess similar DNA-binding domains, yet exert opposing influence on cell proliferation.[26,27] In addition, Klf4 and Klf5 regulate diverse functions, such as cell cycle progression, stem cell maintenance, epidermal and corneal barrier formation, epithelial-mesenchymal transition (EMT), and differentiation of diverse tissues.[27–29] In our earlier studies,[24,25] we employed Le-Cre transgene[30] for conditional ablation of *Klf4* and *Klf5*. However, Le-Cre-driven ablation of *Klf4* and *Klf5* is not useful for studying their role in maintenance of the normally formed adult mouse CE. Moreover, hemizygous Le-Cre eyes are prone to develop abnormalities even in the absence of LoxP sites.[31] We overcame these concerns by ablating *Klf4* in a spatiotemporally regulated manner within the CE using ternary transgenic $Klf4^{LoxP/LoxP}$/$Krt12^{rtTA/rtTA}$/*Tet-O-Cre* ($Klf4^{\Delta/\Delta CE}$) mice and discovered that Klf4 promotes CE cell fate by suppressing EMT.[32,33] In this report, we employ a similar approach using ternary transgenic $Klf5^{\Delta/\Delta CE}$ ($Klf5^{LoxP/LoxP}$/$Krt12^{rtTA/rtTA}$/*Tet-O-Cre*) mice to test the hypothesis that the pro-proliferative activities of Klf5 are essential for maintaining adult CE cell homeostasis. The results obtained from this approach suggest that Klf5 contributes to adult CE homeostasis by promoting proliferation in basal cell layers and permeability barrier function in superficial cell layers.

Materials and Methods

Spatiotemporal Ablation of *Klf5* and Barrier Permeability Assessment

Ternary transgenic $Klf5^{LoxP/LoxP}$/$Krt12^{rtTA/rtTA}$/*Tet-O-Cre* mice ($Klf5^{\Delta/\Delta CE}$) were bred on a mixed background by mating $Klf5^{LoxP/LoxP}$ mice with $Krt12^{rtTA/rtTA}$/*Tet-O-Cre* mice as before.[32–35] Cre expression was induced in adult $Klf5^{\Delta/\Delta CE}$ mice by doxycycline administered through chow and intraperitoneal injections (once every 2 weeks) for a duration of at least 1 month. Ternary transgenic littermates fed with normal chow were used as controls. CE permeability was assessed by staining with 2 µL 1% sodium fluorescein for 2 minutes, rinsing with PBS, and imaging under blue light on a slit-lamp biomicroscope equipped with a digital camera. All animal testing was performed in accordance with guidelines set forth by the Institutional Animal Care and Use Committee of the University of Pittsburgh and the ARVO Statement for the Use of Animals in Ophthalmic and Vision Research. The data presented in this report represent at least three independent experiments.

Histology

$Klf5^{\Delta/\Delta CE}$ and control mice were euthanized via carbon dioxide asphyxiation and cervical dislocation, and their eyes were immediately fixed in 4% paraformaldehyde (Electron Microscopy Sciences, Hatfield, PA, USA) in PBS (pH 7.4) for 24 hours at room temperature (RT). Whole globes were embedded in paraffin, and central corneal 5-µm sections were stained with hematoxylin and eosin (H&E) or periodic acid Schiff (PAS) reagent following standard protocols. Sections were viewed with an Olympus BX60 microscope (Olympus America, Inc., Allentown, PA, USA) and captured using a Spot digital camera (Spot Diagnostics Instruments, Inc., Sterling Heights, CA, USA). All images were processed similarly using Adobe Photoshop and Illustrator (Adobe Systems, San Jose, CA, USA).

Isolation of Total RNA, cDNA Synthesis, and Real-Time Quantitative PCR (QPCR)

Total RNA was isolated from dissected control and $Klf5^{\Delta/\Delta CE}$ corneas using EZ-10 Spin Columns (Bio Basic, Inc., Amherst, NY, USA). Approximately 1 µg RNA was used to synthesize cDNA using mouse moloney leukemia virus reverse transcriptase (Promega, Madison, WI, USA). Transcript levels for target genes were quantified in triplicate using TaqMan or SYBR Green chemistries in an ABI StepOne Plus thermocycler with standardized gene-specific probes and primers. Pyruvate carboxylase (Pcx) and Gapdh served as endogenous controls, respectively. The sequence of oligonucleotide primers used for SYBR Green-based QPCR is provided in Supplementary Table S1.

Antibodies

All antibodies have been previously shown to be cross-reactive to mouse and specific to the desired antigen. A list of antibodies used can be found in Supplementary Table S2.

Immunofluorescent Staining

Eyes from $Klf5^{\Delta/\Delta CE}$ and control mice were embedded in optimal cutting temperature (OCT) medium (Fisher HealthCare, Houston, TX, USA). Thin (8 µm) sections were fixed in 4% paraformaldehyde for 15 minutes, washed twice for 5 minutes in PBS, permeabilized in 0.25% Triton X-100 in PBS for 20 minutes, washed twice for 5 minutes in PBS, treated with 0.1 M glycine in PBS for 30 minutes, washed thrice for 5 minutes with PBS, blocked samples in 10% goat or donkey serum, incubated in primary antibodies diluted in 10% serum overnight at 4°C, washed thrice for 5 minutes in PBS, incubated in appropriate secondary antibody, washed twice for 5 minutes in PBS + 0.1% Tween-20 (PBS-T), counterstained with 4′,6-diamidino-2-phenylindole (DAPI) for 10 minutes, washed twice for 5 minutes in PBS-T, and mounted with AquaMount (Thermo-Fisher Scientific, Pittsburgh, PA, USA). Confocal images were taken on an Olympus IX81 microscope (Olympus America, Inc.). Using Olympus FluoView and Adobe Photoshop and Illustrator, background was identically removed. Proliferative index (PI) was calculated by dividing the number of $Ki67^{+}$ cells by the total cell count, as well as by dividing the $Ki67^{+}$ cells by the length of the base of the CE in one microscopic field. The relative fluorescence intensity was quantified using MetaMorph software (Molecular Devices, LLC, Sunnyvale, CA, USA) in multiple fields from different sections stained independently. Results presented are representative of at least three independent experiments.

Whole-Mount Corneal Staining

The control and $Klf5^{\Delta/\Delta CE}$ eyes were fixed in 4% paraformaldehyde in PBS for 40 minutes at 4°C and washed twice for 20 minutes in PBS. Corneas were dissected and blocked in 2% bovine serum albumin (BSA) and 3% goat serum for 1 hour, washed once for 10 minutes in PBS, incubated in primary antibodies diluted in 2% BSA in PBS overnight at 4°C, washed thrice for 10 minutes in PBS, incubated in secondary antibody diluted in 2% BSA in PBS for 2 hours, adding 1 µg/mL DAPI after the first hour, and washed twice for 20 minutes in PBS. Radial slits were cut, and corneas were mounted with AquaMount.

Investigative Ophthalmology & Visual Science

Images are of the anterior-most 30 μm of the cornea obtained and processed in a similar manner to sectioned immunofluorescent samples.

Western Blotting and Gel Staining

Dissected control and $Klf5^{\Delta/\Delta CE}$ corneas were lysed in radioimmunoprecipitation assay (RIPA) buffer (50 mM Tris-HCl, 150 mM NaCl, 0.5% sodium deoxycholic acid, 1% Triton X-100, and protease inhibitors) or urea (8.0 M urea, 0.8% Triton X-100, 0.2% SDS, 3% β-mercaptoethanol, and protease inhibitors) buffer. Lysates were centrifuged to remove debris, and equal volume of supernatant was separated on 4% to 12% gradient polyacrylamide gels using 3-(N-morpholino)propanesulfonic acid (MOPS) buffer. For staining, gels were washed in water for 1 hour, stained in EZ-Run Protein Staining Solution (Fisher BioReagents, Fair Lawn, NJ, USA) for 2 hours, de-stained in water overnight, and imaged on an Epson 4490 Photo scanner (Epson America, Inc., Long Beach, CA, USA). For Western blotting, gels were transferred to polyvinylidene difluoride (PVDF) membranes, blocked in Odyssey Blocking Buffer (LI-COR Biosciences, Lincoln, NE, USA) for 1 hour, washed thrice for 5 minutes in PBS-T, incubated in primary antibodies diluted in blocking solution and PBS-T overnight at 4°C, washed thrice for 5 minutes in PBS-T, incubated in fluorescently labeled secondary antibodies, washed thrice for 5 minutes in PBS-T, washed once for 5 minutes in PBS, and imaged on an Odyssey scanner (LI-COR Biosciences). Densitometric analyses were performed using Image-J software (National Institutes of Health, Bethesda, MD, USA). β-actin served as loading control for normalization.

Transient Cotransfection Assays

Gastrokine-1 (GKN1)-Luc reporter plasmids, wherein −479/+16 bp, −185/+16 bp, or −113/+16 bp *GKN1* promoter fragments drive luciferase gene expression, were generated by cloning the corresponding PCR-amplified promoter fragments in pGL3-Basic (Promega). Expression vectors pCI, pCI-KLF4, pCI-KLF5, and pCI-OCT1 were from Open Biosystems (Huntsville, AL, USA). Human skin NCTC-2544 epithelial cells[36] were grown in Dulbecco's modified Eagle's medium (DMEM) supplemented with 10% fetal bovine serum in humidified air with 5% CO_2 at 37°C. NCTC cells in midlog phase of growth were cotransfected with 1.83 μg plasmids (0.6 μg GKN1-Luc reporter + 0.4 μg pCI-KLF4, pCI-KLF5, and/or pCI-OCT1, along with 0–1.2 μg pCI as filler to keep the total amount of plasmid used constant, and 30 ng pRL-SV40 plasmid for normalizing the transfection efficiency) using 6 μL FuGENE-6 (Roche Molecular Biochemicals, Indianapolis, IN, USA). After 2 days of transfection, the cells were washed with cold PBS, lysed with 500 μL passive lysis buffer (Promega), and 100 μg lysate was analyzed using a dual luciferase assay kit (Promega and Biotek Synergy-II microplate reader (Biotek, Winooski, VT, USA), integrating the measurement over 10 seconds with a delay of 2 seconds.

Results

Klf5 Is Ablated in a Spatiotemporal Manner in $Klf5^{\Delta/\Delta CE}$ CE

To determine the role of Klf5 in adult mouse CE homeostasis, *Klf5* was ablated in 8-week-old $Klf5^{\Delta/\Delta CE}$ CE using a doxycycline-induced ternary transgenic Tet-On system.[34,35] *Klf5* transcript level within the $Klf5^{\Delta/\Delta CE}$ corneas was decreased to 23% of that in the control, indicating efficient ablation of *Klf5* after 1 month of doxycycline administration (Fig. 1A). While the control and the $Klf5^{\Delta/\Delta CE}$ eyes appeared similar upon visual examination, $Klf5^{\Delta/\Delta CE}$ eyes displayed increased fluorescein staining, indicating decreased permeability barrier function (Fig. 1B). Histological examination of PAS-stained sections revealed fewer cell layers in $Klf5^{\Delta/\Delta CE}$ CE than in control CE, as well as a disrupted CE basement membrane (Fig. 1C). On average, the $Klf5^{\Delta/\Delta CE}$ CE possessed 4.25 cell layers compared with 6.0 in the age-matched controls ($n = 8$; $P = 0.00013$). Examination of the soluble protein profile from the control and the $Klf5^{\Delta/\Delta CE}$ corneas revealed no striking difference, with the expression of corneal crystallins Aldh3a1 and Tkt remaining unaltered (Fig. 1D). Together, these results suggest that though the $Klf5^{\Delta/\Delta CE}$ corneas display decreased number of cell layers, their epithelial properties may remain unperturbed.

Cell Proliferation Rate Is Decreased in Adult $Klf5^{\Delta/\Delta CE}$ CE

Considering that (1) the $Klf5^{\Delta/\Delta CE}$ CE harbored fewer cell layers (Fig. 1C) and (2) Klf5 is known to promote cell proliferation in multiple tissues,[37–40] we tested if cell proliferation is perturbed within the $Klf5^{\Delta/\Delta CE}$ CE. Immunofluorescent stain with anti-Ki67 antibody revealed a significant decrease in the number of proliferating cells in the $Klf5^{\Delta/\Delta CE}$ CE compared with that in the control (Fig. 2A). The PI, defined as the number of $Ki67^+$ cells per total number of cells in each microscopic field or unit length of the cornea, was significantly lower for $Klf5^{\Delta/\Delta CE}$ corneas than the control (Fig. 2B). This correlates well with the $Klf5^{\Delta/\Delta CE}$ CE histology, which shows decreased cell layers (Fig. 1C). As Klf5 regulates human bladder cancer cell proliferation through cyclin-D1,[27,38] we next tested if cyclin-D1 expression is altered in the $Klf5^{\Delta/\Delta CE}$ CE. Immunofluorescent staining for cyclin-D1 indicated decreased expression in the absence of Klf5 (Fig. 3A). Consistent with these results, the expression of phospho(S-10)-p27/Kip1 was upregulated in the $Klf5^{\Delta/\Delta CE}$ CE (Fig. 3B). Together, these results suggest that the decreased $Klf5^{\Delta/\Delta CE}$ cell proliferation is a consequence of downregulation of cyclin-D1 and upregulation of phospho(S-10)-p27/Kip1.

CE Basement Membrane Is Disrupted in $Klf5^{\Delta/\Delta CE}$ Corneas

As histological examination of the PAS-stained sections suggested a disruption in the $Klf5^{\Delta/\Delta CE}$ CE basement membrane (Fig. 1C), we next examined the expression of basement membrane laminins. Immunofluorescent stain with a pan-laminin antibody (raised against laminins from sarcoma, and known to detect basement membrane laminins[41]) detected robust expression of laminins in the control basement membrane but not the $Klf5^{\Delta/\Delta CE}$, demonstrating that the $Klf5^{\Delta/\Delta CE}$ CE basement membrane is disrupted (Fig. 4A). Consistent with these results, *Lama3* and *Lamb1-1* transcript levels were significantly decreased in the $Klf5^{\Delta/\Delta CE}$ compared with the control corneas (Fig. 4B), while the other laminin monomers tested were not altered.

Dsg1a Expression Is Downregulated in the $Klf5^{\Delta/\Delta CE}$ CE

To determine if inefficient cell–cell adhesion led to enhanced cell sloughing resulting in the observed $Klf5^{\Delta/\Delta CE}$ CE thinning (Fig. 1C), we next evaluated the expression of desmosomal components. *Dsg1a* transcripts were significantly decreased to 9% of the control levels, while the transcripts encoding several other desmosomal components were moderately affected in

Investigative Ophthalmology & Visual Science

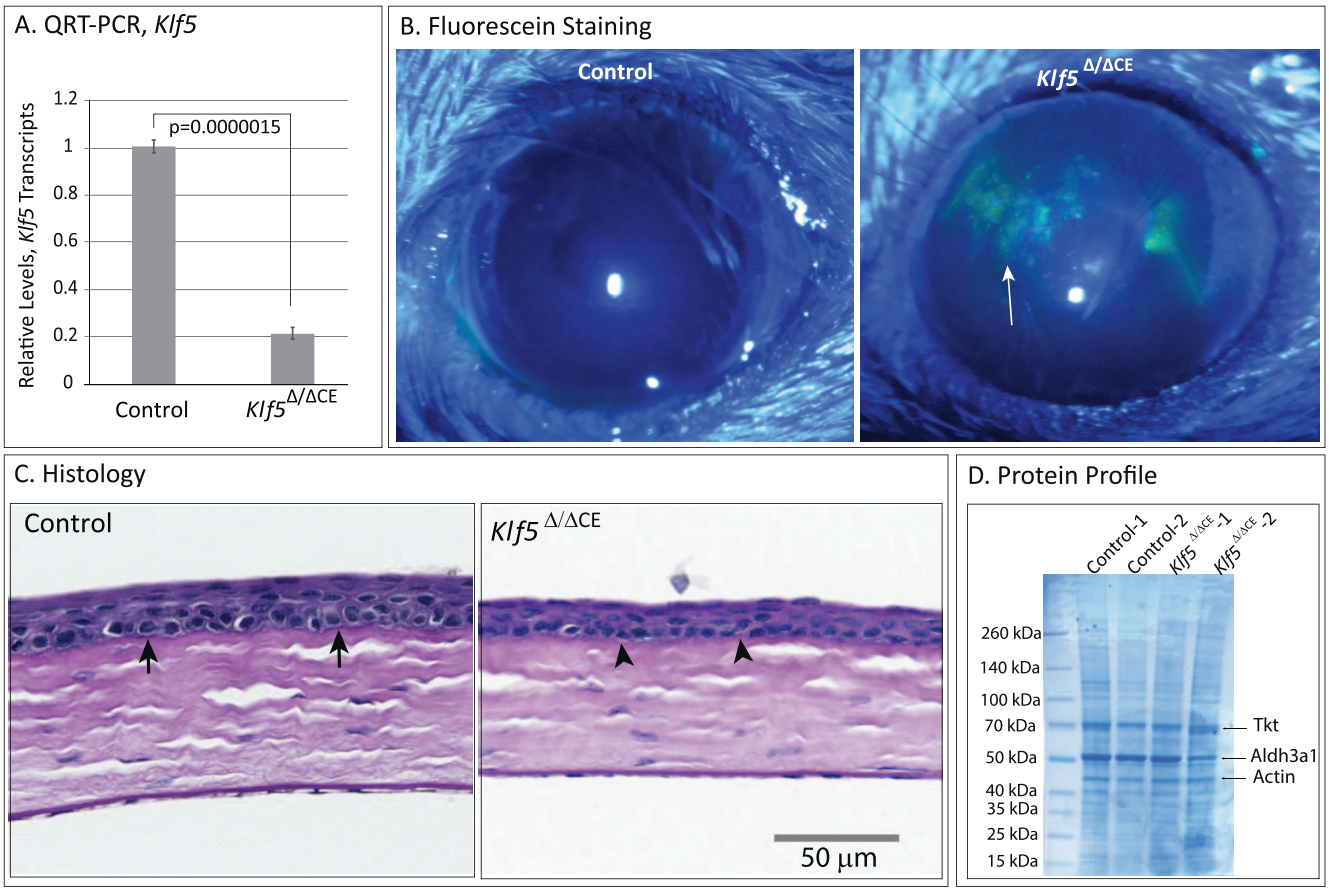

Figure 1. Adult mouse CE-specific ablation of *Klf5* results in fewer cell layers and disrupted barrier function. (**A**) QPCR results demonstrate that *Klf5* transcripts are downregulated to 23% of the control in $Klf5^{\Delta/\Delta CE}$ after 1 month of doxycycline administration ($n = 8$). *Error bars* represent 1 SEM. (**B**) Fluorescein staining revealed green patches in $Klf5^{\Delta/\Delta CE}$ but not control corneas, indicating a loss in $Klf5^{\Delta/\Delta CE}$ barrier function ($n = 5$). (**C**) PAS-stained $Klf5^{\Delta/\Delta CE}$ corneal sections show fewer CE layers as compared to control ($n = 5$). PAS stain also reveals intact basement membrane in the control (*arrows*) but not the $Klf5^{\Delta/\Delta CE}$ (*arrowheads*) corneas. (**D**) Coomassie blue-stained SDS-PAGE profile of soluble protein from two control and $Klf5^{\Delta/\Delta CE}$ corneas each revealed no appreciable change in corneal crystallins Aldh3a1 and Tkt.

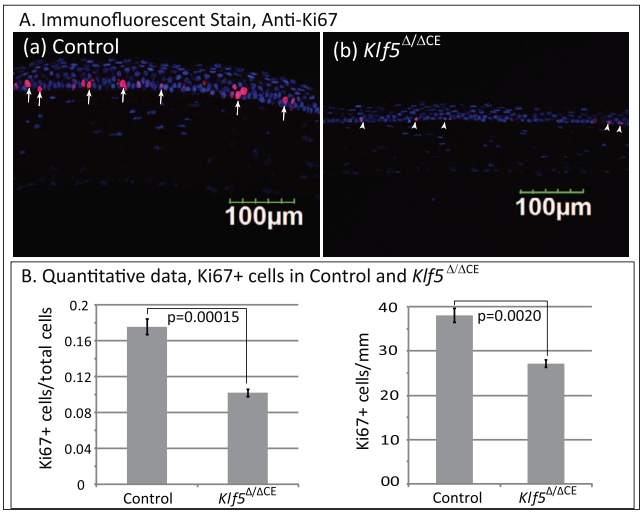

Figure 2. Decreased cell proliferation in $Klf5^{\Delta/\Delta CE}$. (**A**) Immunofluorescent stain with anti-Ki67 antibody revealed an abundance of proliferating cells in the central CE of the control (*arrows*) but not the $Klf5^{\Delta/\Delta CE}$ (*arrowheads*) corneas. (**B**) PI calculated as either number of $Ki67^{+}$ cells per total number of CE cells, or number of $Ki67^{+}$ cells per unit length of the central cornea, reveals a significant decrease in PI in $Klf5^{\Delta/\Delta CE}$ corneas ($n = 13$). *Error bars* represent 1 SEM.

the $Klf5^{\Delta/\Delta CE}$ CE (Fig. 5A). Consistent with these results, immunoblots and immunofluorescent stain revealed downregulation of Dsg1 expression (Figs. 5B, 5C). Taken together, these results suggest that the downregulation of Dsg1a likely contributes to the altered $Klf5^{\Delta/\Delta CE}$ CE barrier function.

Klf5 Maintains Tight Junction in the Adult Mouse CE

To further determine the molecular basis for disrupted barrier function in $Klf5^{\Delta/\Delta CE}$ corneas, we evaluated the expression of tight junction-associated proteins. QPCR demonstrated a significant decrease in *uroplakin* (*Upk*)*1b, Upk3b, Gkn1,* and *Tjp1* transcript levels in the $Klf5^{\Delta/\Delta CE}$ (Fig. 6A). This decrease in Tjp1 and Gkn1 in $Klf5^{\Delta/\Delta CE}$ corneas was also evident in whole-mount immunofluorescent staining (Fig. 6B). In addition, Tjp1 and Gkn1 colocalized to the control corneal tight junctions, suggesting potential interaction between these proteins.

To resolve if downregulation of Gkn1 in the $Klf5^{\Delta/\Delta CE}$ CE is a direct consequence of the absence of Klf5, we performed in vitro transient transfection assays in NCTC epithelial cells[36] wherein reporter plasmids with different GKN1 promoter fragments regulating the luciferase reporter gene were cotransfected with plasmids overexpressing KLF4, KLF5, and/or OCT1. The –479/+16 bp GKN1 promoter activity was stimulated 7.6-, 19- and 2.75-fold by overexpression of KLF4,

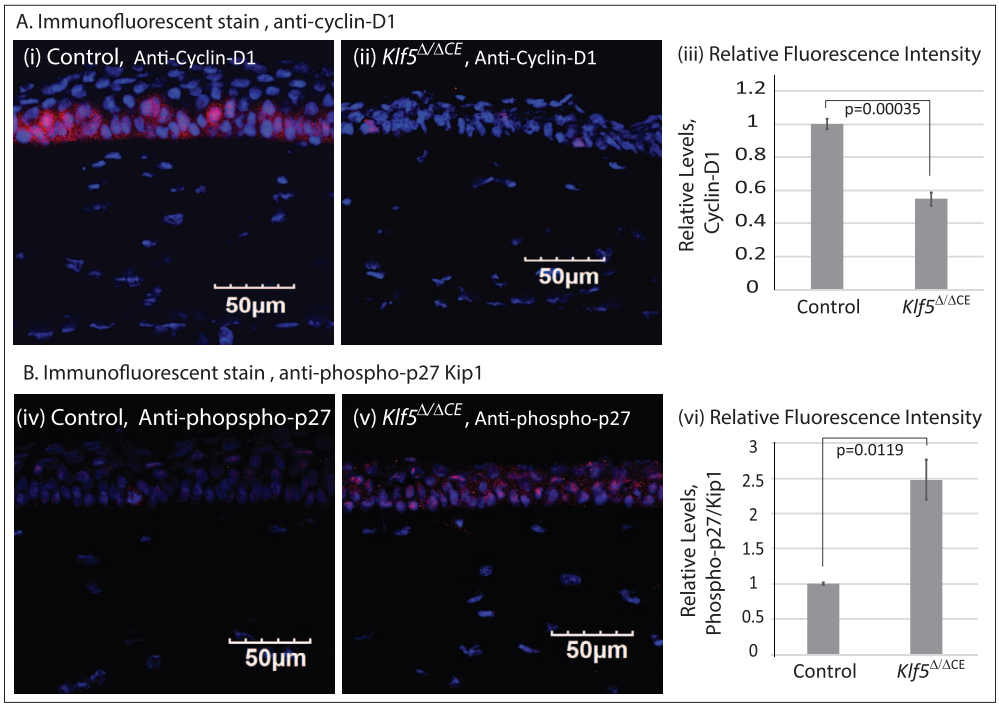

Figure 3. *Klf5*$^{\Delta/\Delta CE}$ corneas display altered expression of cyclin-D1 and phosphor-p27 Kip1. (**A**) Immunofluorescent stain with anti-cyclin-D1 antibody shows control basal epithelial cells display robust expression of cyclin-D1 that is missing in the *Klf5*$^{\Delta/\Delta CE}$ corneas. Relative fluorescence intensity measurement revealed a significant decrease in cyclin-D1 expression in *Klf5*$^{\Delta/\Delta CE}$ corneas ($n = 4$). (**B**) Immunofluorescent stain with anti-phospho(S-10)-p27/Kip1 antibody reveals that the control basal epithelial cells do not express phospho-p27/Kip1, unlike *Klf5*$^{\Delta/\Delta CE}$ CE. Relative fluorescence intensity measurement revealed a significant increase in phospho-p27/Kip1 expression in *Klf5*$^{\Delta/\Delta CE}$ ($n = 4$). *Error bars* represent 1 SEM.

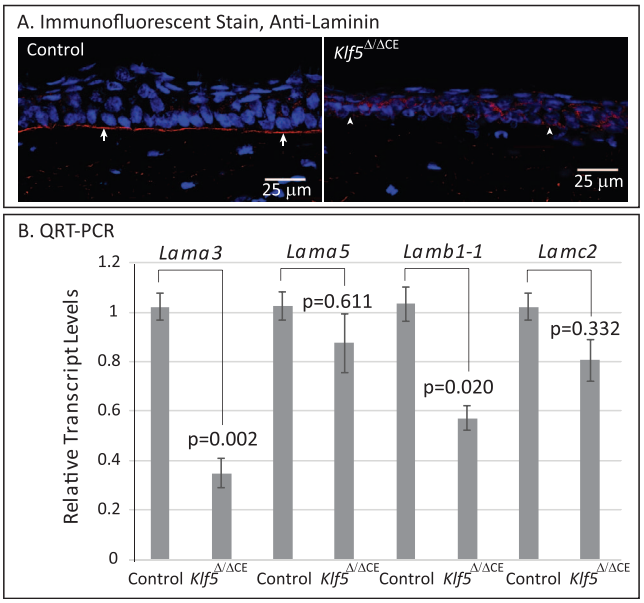

Figure 4. *Klf5*$^{\Delta/\Delta CE}$ corneas display disrupted basement membrane. (**A**) Immunofluorescent staining of control and *Klf5*$^{\Delta/\Delta CE}$ corneas with a pan-laminin antibody reveals that the *Klf5*$^{\Delta/\Delta CE}$ basement membrane is disrupted. Laminin expression was detected underneath the control CE (*arrows*) but not in the *Klf5*$^{\Delta/\Delta CE}$ (*arrowheads*), suggesting that the *Klf5*$^{\Delta/\Delta CE}$ basement membrane is disrupted. (**B**) QPCR reveals a decrease in *Lama3* and *Lamb1-1* transcripts, while other laminin monomers tested remain unchanged ($n = 6$). *Error bars* represent 1 SEM.

KLF5, and OCT1, respectively (Fig. 7). A synergistic effect was observed with cotransfection of OCT1 and KLF5, but not KLF4 and KLF5, or OCT1 and KLF4. Although the extent of stimulation by KLF5 was decreased to 5.5- and 8-fold with shorter −185/+16 bp and −113/+16 bp GKN1 promoter fragments, similar synergism was observed with cotransfection of KLF5 and OCT1, suggesting that the KLF5- and OCT1-responsive elements are present within the −113/+13-bp proximal promoter (Fig. 7). Inclusion of KLF4 erased the synergistic effect observed with KLF5 and OCT1, suggesting that KLF4 competes for the same binding site as KLF5, but does not cooperate with OCT1 (Fig. 7).

Ablation of *Klf5* Does Not Significantly Alter the Expression of CE Markers

In view of our recent finding that the spatiotemporally regulated ablation of the related factor *Klf4* in adult CE results in EMT,[32] it was imperative that we evaluate the status of the *Klf5*$^{\Delta/\Delta CE}$ epithelial identity. Toward this, we examined the expression of keratin-12, E-cadherin, vimentin, and β-catenin. QPCR revealed insignificant change in *Klf4*, *Krt12*, *E-cadherin*, and *vimentin* transcript levels (Fig. 8A). Consistent with these results, immunoblots demonstrated that Klf4, Krt12, E-cadherin, and β-catenin protein levels were largely unaltered in the *Klf5*$^{\Delta/\Delta CE}$ corneas (Fig. 8B). Additionally, immunofluorescent staining with anti-Krt12, anti-E-cadherin, and anti-β-catenin antibodies revealed no significant change in their expression levels or subcellular localization in *Klf5*$^{\Delta/\Delta CE}$ compared with the control corneas (Fig. 8C). Taken together, these results suggest that the expression of keratin-12, E-cadherin, vimentin, and β-catenin is relatively unperturbed in *Klf5*$^{\Delta/\Delta CE}$, despite

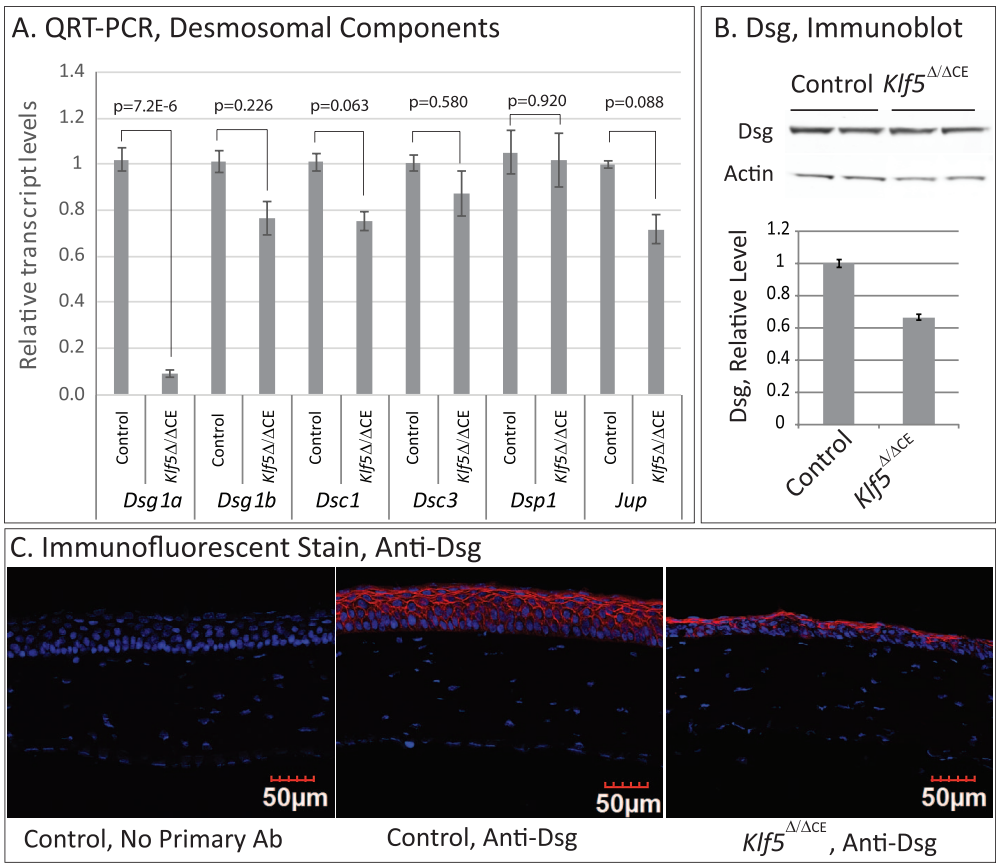

Figure 5. Desmosomal components are altered in *Klf5*$^{\Delta/\Delta CE}$ corneas. (**A**) QPCR shows slight decreases in transcript levels of several desmosomal proteins in *Klf5*$^{\Delta/\Delta CE}$ corneas, as compared to control ($n = 5$). (**B**) Immunoblot shows a decrease in Dsg1 protein expression, with β-actin serving as a loading control for densitometric normalization. (**C**) Immunofluorescent stain with anti-Dsg1 antibody shows an altered expression pattern for *Klf5*$^{\Delta/\Delta CE}$ corneas, with expression limited to the very anterior-most layers ($n = 4$). *Error bars* represent 1 SEM.

decreased rate of proliferation and striking morphological changes.

Discussion

In this report, we provide evidence that Klf5 contributes to the adult CE homeostasis by maintaining optimal rate of CE cell proliferation and promoting cellular junctions based on the results obtained by spatiotemporally regulated ablation of *Klf5*. The *Klf5*$^{\Delta/\Delta CE}$ epithelium displayed defective permeability barrier, decreased proliferation coupled with fewer CE cell layers, and a disrupted basement membrane. Consistent with these results, the expression of tight junction components Tjp1 and Gkn1, desmosomal protein Dsg1, and cell proliferation regulators cyclin-D1 and phospho(Ser-10)p27/Kip1 was altered in the *Klf5*$^{\Delta/\Delta CE}$ CE. Despite significant changes in *Klf5*$^{\Delta/\Delta CE}$ proliferation and barrier function, the expression of Krt12, E-cadherin, and β-catenin remained relatively unaltered. Thus, unlike *Klf4*$^{\Delta/\Delta CE}$, where CE cell proliferation rate was elevated and epithelial properties were lost in favor of mesenchymal features,[32] the *Klf5*$^{\Delta/\Delta CE}$ CE displays diminished cell proliferation while retaining many of their epithelial characteristics. Together, these results are consistent with a functional dichotomy between the structurally related transcription factors Klf4 and Klf5 that work in concert to maintain CE homeostasis (Fig. 9).

Klf4 and Klf5 are among the most highly expressed transcription factors in the mouse CE, where they play essential nonredundant roles.[23–25,42–46] Although Klf4 and Klf5 possess similar DNA-binding domains, they exert opposing influence on cell proliferation.[27,47] Klf4, an inhibitor of cell proliferation, promotes corneal epithelial differentiation by suppressing EMT,[32] while the data presented in this report reveal that Klf5 promotes basal CE cell proliferation. To understand the basis for the nonredundant functions of Klf4 and Klf5 despite their similar DNA-binding domains, it is necessary to determine the molecular constraints that establish distinct DNA-binding sequence specificities on their target gene promoters. Considering the divergent nature of the Klf4 and Klf5 N-terminal regulatory domains, it is conceivable that Klf4- and Klf5-target site selection is influenced by the specific cofactors that they interact with, and/or the sequences flanking the core recognition sequence.

This report demonstrates that Klf5 contributes to the CE permeability barrier function by regulating the expression of tight junction components in superficial cells, desmosomal components in wing cells, and laminins in the basement membrane. Previously, we have shown that Klf5 is relatively more abundant in the basal than the superficial CE cells.[25,42] Disruption of tight junctions within the superficial *Klf5*$^{\Delta/\Delta CE}$ cells suggests a key role for residual Klf5 in the superficial cell layers. Alternatively, this may reflect an indirect outcome of their premature sloughing off—a possibility that is consistent with the weaker desmosomes in the spinous and wing cells. Defects in any of these components that contribute to the structural integrity of the CE are deleterious.[48–50] A similar function was previously attributed to Klf5 in the mouse intestine, where the barrier function

Investigative Ophthalmology & Visual Science

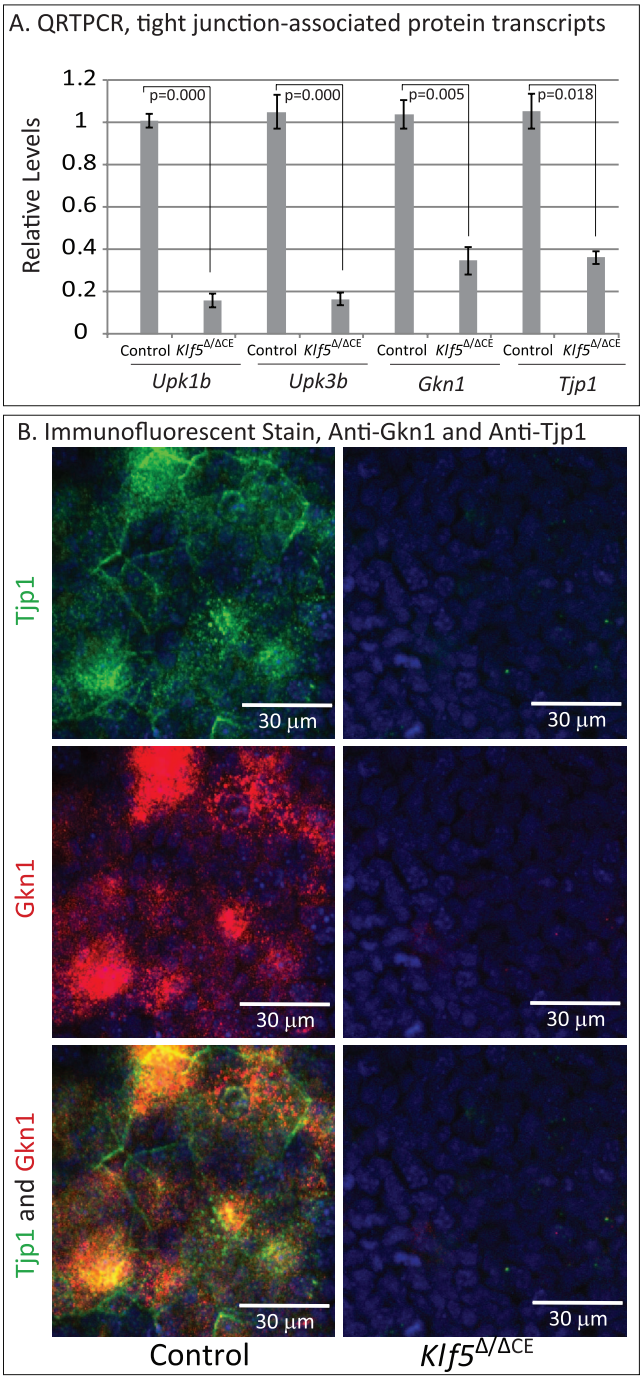

Figure 6. *Klf5*$^{\Delta/\Delta CE}$ corneas show decreased transcription and expression of tight junction proteins. (**A**) QPCR detected significantly less transcripts encoding tight junction-associated *Upk1b, Upk3b, Gkn1,* and *Tjp1* in *Klf5*$^{\Delta/\Delta CE}$ than in control corneas ($n = 6$). *Error bars* represent 1 SEM. (**B**) Whole-mount immunofluorescent staining revealed a sharp decrease in Tjp1 and Gkn1 expression in *Klf5*$^{\Delta/\Delta CE}$ corneas, compared with the control.

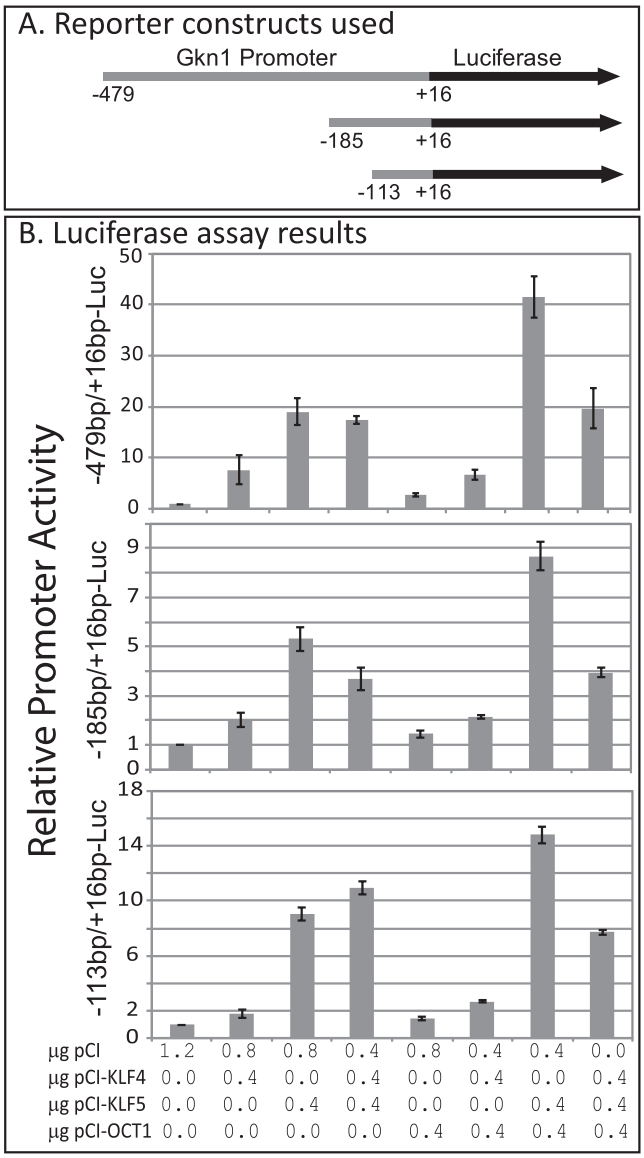

Figure 7. Transient cotransfections indicate the roles of KLF5 and OCT1 in regulating *GKN1* promoter activity. GKN1-Luc reporter plasmids with varying *GKN1* promoter fragment sizes were cotransfected with expression vectors pCI-KLF4, -KLF5, and/or -OCT1. Reporter assays revealed synergistically increased expression upon cotransfection of KLF5 and OCT1. KLF4 and KLF5 appear to bind the same cis-elements as their cotransfection did not result in any additive or synergistic activation. A similar expression pattern was observed in all the promoter fragments tested, suggesting that the KLF5- and OCT1-responsive elements reside within the smallest promoter fragment tested ($n = 3$). *Error bars* represent 1 SEM.

was compromised in the absence of Klf5.[14] Our results also revealed downregulation of Gkn1, Upk-1b and -3b that serve important gastrointestinal and urothelial permeability barrier functions.[51–54] Gkn1, also known as AMP-18, is an 18-kDa secreted protein that serves as a mitogen and helps maintain intestinal epithelial barrier function by stabilizing tight junction proteins occludin and Tjp1.[53,55,56] Corneal functions of Gkn1 remain to be tested though our finding that Gkn1 colocalizes with Tjp1 at the control CE tight junctions suggests a similar role for it in the CE as in the GI tract: to maintain tight junctions.

In transient transfection assays, *GKN1* promoter activity was regulated synergistically by KLF5 and OCT1 in NCTC cells, while KLF4 exerted little influence. OCT1 is a ubiquitously expressed transcription factor that has been implicated in regulating differentiation and preventing tumorigenesis.[57–59]

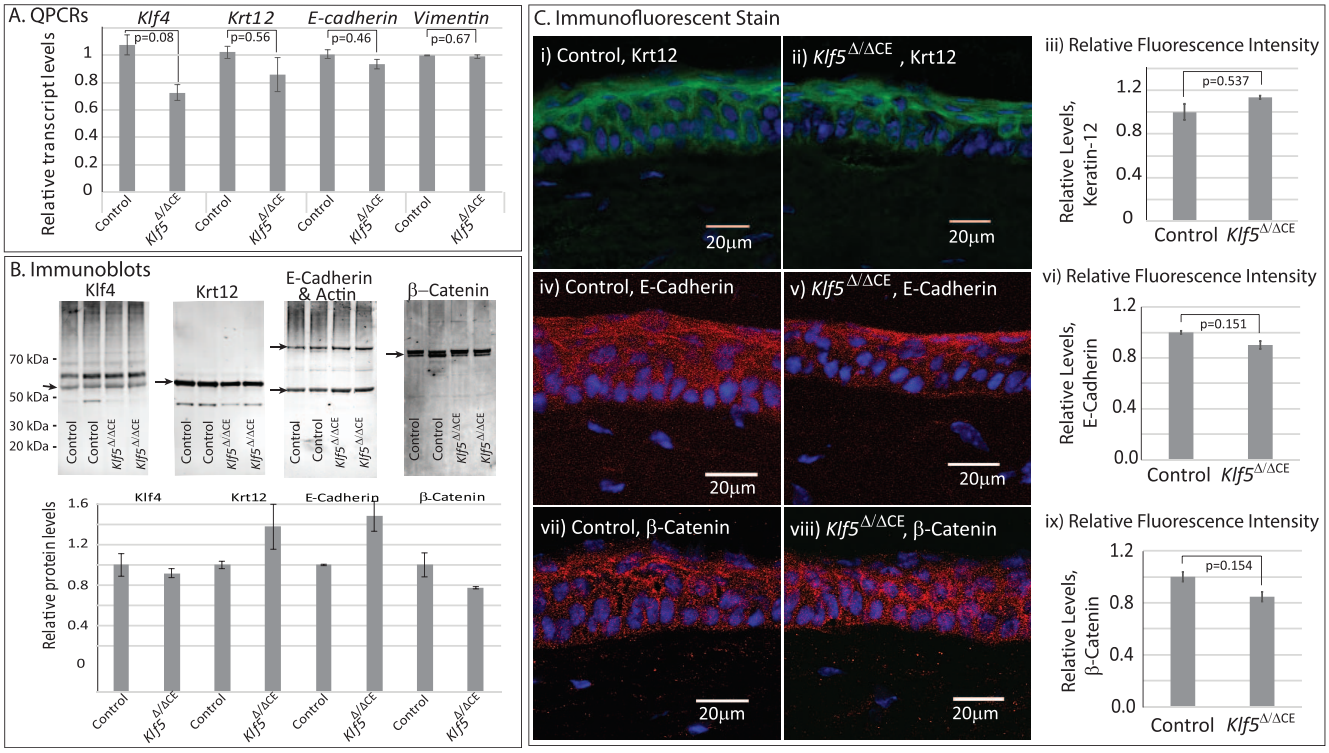

Figure 8. Expression of CE-specific markers remains relatively unchanged in *Klf5*$^{\Delta/\Delta CE}$ corneas. (**A**) QPCR analyses show little change in *Klf4*, *Krt12, E-cadherin*, and *vimentin* transcripts between the control and *Klf5*$^{\Delta/\Delta CE}$ CE ($n = 8$). (**B**) Immunoblots and their densitometric measurements with β-actin as loading control show that Klf4, Krt12, E-cadherin, and β-catenin expression is relatively unchanged in *Klf5*$^{\Delta/\Delta CE}$ corneas, compared with the control. (**C**) Immunofluorescent staining and corresponding fluorescence intensity measurements reveal little change in expression of Krt12, E-cadherin, and β-catenin between *Klf5*$^{\Delta/\Delta CE}$ and control ($n = 3$). *Error bars* represent 1 SEM.

The synergistic effect of KLF5 and OCT1 on *GKN1* promoter activity demonstrates that in addition to its role in basal epithelial cell proliferation, Klf5 is also important for maintaining the properties of differentiated superficial cells. The absence of this synergistic effect when KLF4 and KLF5 were cotransfected suggests that they both compete for the same *cis*-elements within the *GKN1* proximal promoter. Whether Gkn1 is downregulated in the *Klf5*$^{-/-}$ intestinal epithelium, and intestinal expression of *Gkn1* also is regulated by Klf5 in a similar manner as in the CE, remains to be determined. Identification of KLF5- and OCT1-target sites within *GKN1* proximal promoter by chromatin immunoprecipitation, and evaluation of their functional relevance by mutagenesis and transgenic approach, would be necessary to provide conclusive in vivo evidence for synergistic regulation of *GKN1* by KLF5 and OCT1.

Our data suggest that Klf5 promotes cell proliferation, in part, by upregulating cyclin-D1 expression while suppressing that of phospho(Ser-10)-p27/Kip1, facilitating G1 to S phase transition in cell cycle. This inference, however, is purely correlative, and definitive evidence for direct involvement of KLF5 in regulating cyclin-D1 and p27 expression would require demonstration of binding of KLF5 to the genes encoding cyclin-D1 and p27 in CE, and the resultant change in their corresponding promoter activities. In previous studies, upon Le-Cre mediated pan-ocular surface ablation of *Klf5* from embryonic day 10, the *Klf5*CN CE displayed increased cell proliferation,[25] in contrast with the results presented here. Corneal neovascularization and the influx of immune cells evident within the *Klf5*CN corneas[42] is absent in the present *Klf5*$^{\Delta/\Delta CE}$ corneas, suggesting that the increased cell proliferation in the *Klf5*CN corneas is an indirect outcome of the inflammatory environment generated as a result of the pan-ocular surface ablation of *Klf5* from an early embryonic stage.[25,42] The decreased *Klf5*$^{\Delta/\Delta CE}$ CE cell proliferation is consistent with basal epithelial cell-preferred expression of Klf5, and its well-established pro-proliferative activity in diverse cell types.[38,47,60]

In summary, we have ablated *Klf5* in the adult mouse CE to better understand the role of this transcription factor in maintaining corneal homeostasis. Our findings suggest Klf5 is essential for proper barrier function and CE cell proliferation. Several studies report epithelial differentiation is reliant on a balance between Klf5 and Klf4 both spatially and temporally.[29,61–63] In the intestinal epithelium, Klf5 localizes in crypts, where cells are actively dividing, and Klf4 is concentrated at the tops of intestinal villi, where cells are differentiated.[47,64,65] Similarly, corneal epithelial Klf5 is most highly expressed in the basal cells, and Klf4 is relatively more abundant in the superficial cells,[25,33] Given the decreased *Klf5*$^{\Delta/\Delta CE}$ cell proliferation, it is reasonable to speculate that Klf4 and Klf5 have similar functions in the CE as they do in intestinal epithelium, regarding proliferation and differentiation. Our results presented in this report, coupled with previous data,[32,33] reveal that the choice between CE cell proliferation and differentiation is determined by the delicate balance between the anti- and pro-proliferative activities of Klf4 and Klf5, respectively (Fig. 9). When this balance is perturbed, CE homeostasis is disrupted resulting in diseases, such as ocular surface squamous metaplasia and neoplasia.

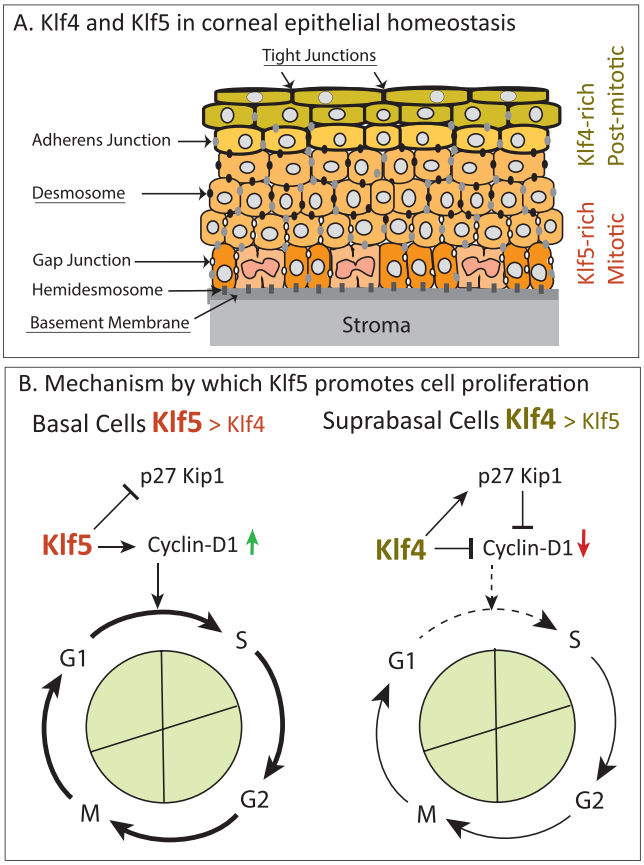

Figure 9. Schematic representation of our findings and a model suggesting functional dichotomy between structurally related Klf4 and Klf5. (**A**) The results presented in this manuscript demonstrate that Klf5 contributes to the formation of permeability barrier at the apical surface of the cornea, desmosomal junctions at the cell–cell boundaries, and basement membrane (*underlined*), in addition to ensuring a pro-proliferative environment in the basal cell layers, without affecting the expression of critical CE-cell markers, such as Krt12, E-cadherin, and β-catenin. We propose that the choice between CE cell proliferation and differentiation is determined by the delicate balance between the anti- and pro-proliferative activities of Klf4 and Klf5, respectively. Basal epithelial cells enriched in Klf5 are in a pro-proliferative environment, while the wing cells and superficial cells are enriched in Klf4 and are in a postmitotic, prodifferentiation environment. This balance is perturbed in CE diseases, such as squamous metaplasia and ocular surface squamous neoplasia. (**B**) Mechanism by which Klf5 promotes cell proliferation. Our results show that Klf5 promotes cell proliferation, in part, by upregulating cyclin-D1 expression while suppressing that of phospho-p27(Ser-10)/Kip1, facilitating G1 to S phase transition in cell cycle. Previous studies from our lab and others suggest that Klf4 has opposite effects on cyclin, suppressing cell proliferation and creating a prodifferentiation environment in the suprabasal cell layers.

Acknowledgments

The authors thank Kate Davoli (Tissue Culture and Histology Core Module) for help with histology, and Kira Lathrop (Imaging Core Module) for help with imaging.

Supported by National Institutes of Health grant R01 EY026533 (SKS), National Eye Institute Core Grant P30 EY08098, and by unrestricted grants from Research to Prevent Blindness and the Eye and Ear Foundation of Pittsburgh.

Disclosure: **C.L. Loughner**, None; **A. Tiwari**, None; **D. Kenchegowda**, None; **S. Swamynathan**, None; **S.K. Swamynathan**, None

References

1. Jester JV, Moller-Pedersen T, Huang J, et al. The cellular basis of corneal transparency: evidence for 'corneal crystallins.' *J Cell Sci*. 1999;112(pt 5):613–622.
2. Piatigorsky J. Enigma of the abundant water-soluble cytoplasmic proteins of the cornea: the "refracton" hypothesis. *Cornea*. 2001;20:853–858.
3. Hassell JR, Birk DE. The molecular basis of corneal transparency. *Exp Eye Res*. 2010;91:326–335.
4. Azar DT. Corneal angiogenic privilege: angiogenic and antiangiogenic factors in corneal avascularity, vasculogenesis, and wound healing (an American Ophthalmological Society thesis). *Trans Am Ophthalmol Soc*. 2006;104:264–302.
5. Niederkorn JY, Stein-Streilein J. History and physiology of immune privilege. *Ocul Immunol Inflamm*. 2010;18:19–23.
6. Barabino S, Chen Y, Chauhan S, Dana R. Ocular surface immunity: homeostatic mechanisms and their disruption in dry eye disease. *Prog Retin Eye Res*. 2012;31:271–285.
7. Clements JL, Dana R. Inflammatory corneal neovascularization: etiopathogenesis. *Semin Ophthalmol*. 2011;26:235–245.
8. Dhouailly D, Pearton DJ, Michon F. The vertebrate corneal epithelium: from early specification to constant renewal. *Dev Dyn*. 2014;243:1226–1241.
9. Swamynathan SK. Ocular surface development and gene expression. *J Ophthalmol*. 2013;2013:103947.
10. Sartaj R, Chee RI, Yang J, et al. LIM homeobox domain 2 is required for corneal epithelial homeostasis. *Stem Cells*. 2016;34:493–503.
11. Koppaka V, Chen Y, Mehta G, et al. ALDH3A1 plays a functional role in maintenance of corneal epithelial homeostasis. *PLoS One*. 2016;11:e0146433.
12. Soriano-Romani L, Garcia-Posadas L, Lopez-Garcia A, Paraoan L, Diebold Y. Thrombospondin-1 induces differential response in human corneal and conjunctival epithelial cells lines under in vitro inflammatory and apoptotic conditions. *Exp Eye Res*. 2015;134:1–14.
13. Ouyang H, Xue Y, Lin Y, et al. WNT7A and PAX6 define corneal epithelium homeostasis and pathogenesis. *Nature*. 2014;511:358–361.
14. McConnell BB, Kim SS, Yu K, et al. Kruppel-like factor 5 is important for maintenance of crypt architecture and barrier function in mouse intestine. *Gastroenterology*. 2011;141:1302–1313.
15. Gaddipati S, Rao P, Jerome AD, Burugula BB, Gerard NP, Suvas S. Loss of neurokinin-1 receptor alters ocular surface homeostasis and promotes an early development of herpes stromal keratitis. *J Immunol*. 2016;197:4021–4033.
16. Ng GY, Yeh LK, Zhang Y, et al. Role of SH2-containing tyrosine phosphatase Shp2 in mouse corneal epithelial stratification. *Invest Ophthalmol Vis Sci*. 2013;54:7933–7942.
17. Jeong S, Ledee DR, Gordon GM, et al. Interaction of clusterin and matrix metalloproteinase-9 and its implication for epithelial homeostasis and inflammation. *Am J Pathol*. 2012;180:2028–2039.
18. Stephens DN, Klein RH, Salmans ML, Gordon W, Ho H, Andersen B. The Ets transcription factor EHF as a regulator of cornea epithelial cell identity. *J Biol Chem*. 2013;288:34304–34324.
19. McDade SS, Henry AE, Pivato GP, et al. Genome-wide analysis of p63 binding sites identifies AP-2 factors as co-regulators of epidermal differentiation. *Nucleic Acids Res*. 2012;40:7190–7206.
20. Kinoshita S, Adachi W, Sotozono C, et al. Characteristics of the human ocular surface epithelium. *Prog Retin Eye Res*. 2001;20:639–673.

21. Klintworth GK. The molecular genetics of the corneal dystrophies—current status. *Front Biosci*. 2003;8:d687–713.
22. Xiao B, Wang Y, Reinach PS, et al. Dynamic ocular surface and lacrimal gland changes induced in experimental murine dry eye. *PLoS One*. 2015;10:e0115333.
23. Norman B, Davis J, Piatigorsky J. Postnatal gene expression in the normal mouse cornea by SAGE. *Invest Ophthalmol Vis Sci*. 2004;45:429–440.
24. Swamynathan SK, Katz JP, Kaestner KH, Ashery-Padan R, Crawford MA, Piatigorsky J. Conditional deletion of the mouse Klf4 gene results in corneal epithelial fragility, stromal edema, and loss of conjunctival goblet cells. *Mol Cell Biol*. 2007;27:182–194.
25. Kenchegowda D, Swamynathan S, Gupta D, Wan H, Whitsett J, Swamynathan SK. Conditional disruption of mouse Klf5 results in defective eyelids with malformed meibomian glands, abnormal cornea and loss of conjunctival goblet cells. *Dev Biol*. 2011;356:5–18.
26. Swamynathan SK. Kruppel-like factors: three fingers in control. *Hum Genomics*. 2010;4:263–270.
27. Ghaleb AM, Nandan MO, Chanchevalap S, Dalton WB, Hisamuddin IM, Yang VW. Kruppel-like factors 4 and 5: the yin and yang regulators of cellular proliferation. *Cell Res*. 2005;15:92–96.
28. Yang Y, Goldstein BG, Chao HH, Katz JP. KLF4 and KLF5 regulate proliferation, apoptosis and invasion in esophageal cancer cells. *Cancer Biol Ther*. 2005;4:1216–1221.
29. Aksoy I, Giudice V, Delahaye E, et al. Klf4 and Klf5 differentially inhibit mesoderm and endoderm differentiation in embryonic stem cells. *Nat Commun*. 2014;5:3719.
30. Ashery-Padan R, Marquardt T, Zhou X, Gruss P. Pax6 activity in the lens primordium is required for lens formation and for correct placement of a single retina in the eye. *Genes Dev*. 2000;14:2701–2711.
31. Dora NJ, Collinson JM, Hill RE, West JD. Hemizygous Le-Cre transgenic mice have severe eye abnormalities on some genetic backgrounds in the absence of LoxP sites. *PLoS One*. 2014;9:e109193.
32. Tiwari A, Loughner CL, Swamynathan S, Swamynathan SK. KLF4 plays an essential role in corneal epithelial homeostasis by promoting epithelial cell fate and suppressing epithelial-mesenchymal transition. *Invest Ophthalmol Vis Sci*. 2017;58:2785–2795.
33. Delp EE, Swamynathan S, Kao WW, Swamynathan SK. Spatiotemporally regulated ablation of Klf4 in adult mouse corneal epithelial cells results in altered epithelial cell identity and disrupted homeostasis. *Invest Ophthalmol Vis Sci*. 2015;56:3549–3558.
34. Chikama T, Hayashi Y, Liu CY, et al. Characterization of tetracycline-inducible bitransgenic Krt12rtTA/+/tet-O-LacZ mice. *Invest Ophthalmol Vis Sci*. 2005;46:1966–1972.
35. Chikama T, Liu CY, Meij JT, et al. Excess FGF-7 in corneal epithelium causes corneal intraepithelial neoplasia in young mice and epithelium hyperplasia in adult mice. *Am J Pathol*. 2008;172:638–649.
36. Neufahrt A, Forster FJ, Gottschalk K, Leonhardi G. Long-term tissue culture of epithelial-like cells from human skin (NCTC strain 2544). II. Viscosity changes after enzyme treatment. *Arch Dermatol Res*. 1978;261:27–31.
37. Sun R, Chen X, Yang VW. Intestinal-enriched Kruppel-like factor (Kruppel-like factor 5) is a positive regulator of cellular proliferation. *J Biol Chem*. 2001;276:6897–6900.
38. Chen C, Benjamin MS, Sun X, et al. KLF5 promotes cell proliferation and tumorigenesis through gene regulation and the TSU-Pr1 human bladder cancer cell line. *Int J Cancer*. 2006;118:1346–1355.
39. Liu R, Zhou Z, Zhao D, Chen C. The induction of KLF5 transcription factor by progesterone contributes to progesterone-induced breast cancer cell proliferation and dedifferentiation. *Mol Endocrinol*. 2011;25:1137–1144.
40. Shi HJ, Wen JK, Miao SB, Liu Y, Zheng B. KLF5 and hhLIM cooperatively promote proliferation of vascular smooth muscle cells. *Mol Cel Biochem*. 2012;367:185–194.
41. Satz JS, Barresi R, Durbeej M, et al. Brain and eye malformations resembling Walker-Warburg syndrome are recapitulated in mice by dystroglycan deletion in the epiblast. *J Neurosci*. 2008;28:10567–10575.
42. Kenchegowda D, Harvey SAK, Swamynathan S, Lathrop KL, Swamynathan SK. Critical role of Klf5 in regulating gene expression during post-eyelid opening maturation of mouse corneas. *PLoS One*. 2012;7:e44771.
43. Swamynathan S, Buela KA, Kinchington P, et al. Klf4 regulates the expression of Slurp1, which functions as an immunomodulatory peptide in the mouse cornea. *Invest Ophthalmol Vis Sci*. 2012;53:8433–8446.
44. Swamynathan S, Kenchegowda D, Piatigorsky J, Swamynathan SK. Regulation of corneal epithelial barrier function by Kruppel-like transcription factor 4. *Invest Ophthalmol Vis Sci*. 2011;52:1762–1769.
45. Swamynathan SK, Davis J, Piatigorsky J. Identification of candidate Klf4 target genes reveals the molecular basis of the diverse regulatory roles of Klf4 in the mouse cornea. *Invest Ophthalmol Vis Sci*. 2008;49:3360–3370.
46. Young RD, Swamynathan SK, Boote C, et al. Stromal edema in klf4 conditional null mouse cornea is associated with altered collagen fibril organization and reduced proteoglycans. *Invest Ophthalmol Vis Sci*. 2009;50:4155–4161.
47. McConnell BB, Ghaleb AM, Nandan MO, Yang VW. The diverse functions of Kruppel-like factors 4 and 5 in epithelial biology and pathobiology. *Bioessays*. 2007;29:549–557.
48. Takaoka M, Nakamura T, Ban Y, Kinoshita S. Phenotypic investigation of cell junction-related proteins in gelatinous drop-like corneal dystrophy. *Invest Ophthalmol Vis Sci*. 2007;48:1095–1101.
49. Moroi SE, Gokhale PA, Schteingart MT, et al. Clinicopathologic correlation and genetic analysis in a case of posterior polymorphous corneal dystrophy. *Am J Ophthalmol*. 2003;135:461–470.
50. Bower KS, Edwards JD, Wagner ME, Ward TP, Hidayat A. Novel corneal phenotype in a patient with alport syndrome. *Cornea*. 2009;28:599–606.
51. Carpenter AR, Becknell MB, Ching CB, et al. Uroplakin 1b is critical in urinary tract development and urothelial differentiation and homeostasis. *Kidney Int*. 2016;89:612–624.
52. Deng FM, Liang FX, Tu L, et al. Uroplakin IIIb, a urothelial differentiation marker, dimerizes with uroplakin Ib as an early step of urothelial plaque assembly. *J Cell Biol*. 2002;159:685–694.
53. Walsh-Reitz MM, Huang EF, Musch MW, et al. AMP-18 protects barrier function of colonic epithelial cells: role of tight junction proteins. *Am J Physiol Gastrointest Liver Physiol*. 2005;289:G163–G171.
54. Chen P, Li YC, Toback FG. AMP-18 targets p21 to maintain epithelial homeostasis. *PLoS One*. 2015;10:e0125490.
55. Chen P, Bakke D, Kolodziej L, et al. Antrum mucosal protein-18 peptide targets tight junctions to protect and heal barrier structure and function in models of inflammatory bowel disease. *Inflamm Bowel Dis*. 2015;21:2393–2402.
56. Toback FG, Walsh-Reitz MM, Musch MW, et al. Peptide fragments of AMP-18, a novel secreted gastric antrum mucosal protein, are mitogenic and motogenic. *Am J Physiol Gastrointest Liver Physiol*. 2003;285:G344–G353.

Investigative Ophthalmology & Visual Science

57. Hwang SS, Kim LK, Lee GR, Flavell RA. Role of OCT-1 and partner proteins in T cell differentiation. *Biochem Biophys Acta*. 2016;1859:825–831.
58. Shakya A, Cooksey R, Cox JE, Wang V, McClain DA, Tantin D. Oct1 loss of function induces a coordinate metabolic shift that opposes tumorigenicity. *Nat Cell Biol*. 2009;11:320–327.
59. Li Y, Dong M, Kong F, Zhou J. Octamer transcription factor 1 mediates epithelial-mesenchymal transition in colorectal cancer. *Tumour Biol*. 2015;36:9941–9946.
60. Dong JT, Chen C. Essential role of KLF5 transcription factor in cell proliferation and differentiation and its implications for human diseases. *Cel Mol Life Sci*. 2009;66:2691–2706.
61. Ohnishi S, Laub F, Matsumoto N, et al. Developmental expression of the mouse gene coding for the Kruppel-like transcription factor KLF5. *Dev Dyn*. 2000;217:421–429.
62. Dang DT, Pevsner J, Yang VW. The biology of the mammalian Kruppel-like family of transcription factors. *Int J Biochem Cell Biol*. 2000;32:1103–1121.
63. Dang DT, Zhao W, Mahatan CS, Geiman DE, Yang VW. Opposing effects of Kruppel-like factor 4 (gut-enriched Kruppel-like factor) and Kruppel-like factor 5 (intestinal-enriched Kruppel-like factor) on the promoter of the Kruppel-like factor 4 gene. *Nucleic Acids Res*. 2002;30:2736–2741.
64. Kuruvilla JG, Ghaleb AM, Bialkowska AB, Nandan MO, Yang VW. Role of Kruppel-like factor 5 in the maintenance of the stem cell niche in the intestinal crypt. *Stem Cell Trans Invest*. 2015;2:e839.
65. Flandez M, Guilmeau S, Blache P, Augenlicht LH. KLF4 regulation in intestinal epithelial cell maturation. *Exp Cell Res*. 2008;314:3712–3723.

Investigative Ophthalmology & Visual Science